Closed Loop Control of a Six Phase Interleaved Bidirectional dc-dc Boost Converter for an EV/HEV Application

D. Schumacher, P. Magne, *Member*, *IEEE*, M. Preindl, *Member, IEEE*, B. Bilgin, *Member, IEEE*, and A. Emadi, *Fellow, IEEE*
McMaster Automotive Resource Center (MARC)
McMaster University, Hamilton, ON, Canada
E-mail:bilginb@mcmaster.ca

Abstract—**This paper discusses and implements a control strategy for a six-phase interleaved bidirectional dc-dc converter for a battery system for an HEV/EV application. First, basic control strategies of dc-dc converters are reviewed for interleaving and for bidirectional operation. Then, the two-loop average mode current control (AVGCCM) is used along with a unified control strategy for the bidirectional operation. A single unified controller is implemented for bidirectional operation along with active rectification for eliminating the discontinuous conduction mode (DCM). Both, techniques are analyzed in simulation and tested on a 5kW experimental setup.**

I. INTRODUCTION

Electric vehicle applications are gaining fast headway into the transportation market as replacements for conventional internal combustion engine vehicles. Improvements in cost, weight, efficiency, and power density are all important advancements to push EV/HEV applications beyond traditional combustion vehicles. One key facet within most EV/HEV applications is the bidirectional dc-dc converter, which connects the energy storage system to the inverter. During boost mode, power is delivered from the energy storage system (ESS) to the drive system while in buck mode, energy is sent back to the ESS system. This bidirectional power flow enables regenerative braking which improves efficiency [1-3], it provides more voltage flexibility for the ESS and inverter system reducing the size of the ESS and also allowing better control of the drive system by adjusting the input voltage to the inverter. This variability also permits different energy sources like fuel cells, batteries and ultracapacitors to be used, providing a diversity of applications [2-5].

By interleaving multiple phases within the bidirectional converter, further advancements can be made such as the minimization in current rating of the inductor and switches [1-8], reduction in current and voltage ripple at the input and output [5-7], smaller component size [8], improvement in output impedance properties [6], and replacement of aluminum electrolytic capacitors with film or ceramic capacitors to reduce equivalent series resistance and improve power density [5]. However, as the number of phases increase, the number of switches, cost, weight, complexity and size also increase. Therefore, there needs to be a balance when selecting the number of phases for each application. In [1], a six-phase

bidirectional boost converter has been proposed for a high-power application, considering the cost, volume, efficiency, input current ripple and inductor volume using off-the-shelf components. This paper investigates the selection of the control strategy to achieve the desired operation of the multiphase converter.
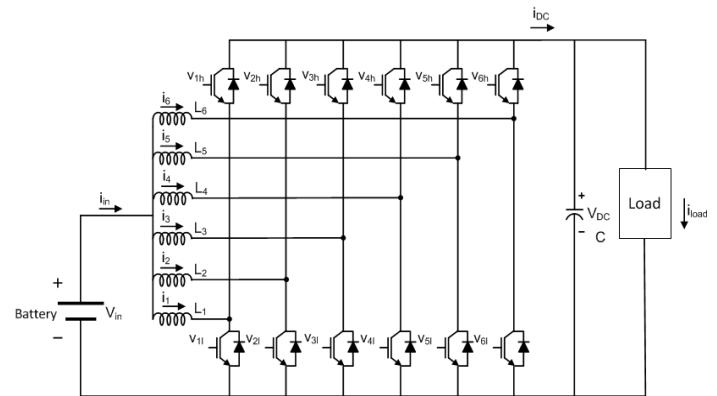

Fig. 1.   6-Phase Interleaved Bidirectional DC/DC Converter.

This paper is structured as follows, first an overview of interleaving multiple phases to achieve equal current sharing is reviewed, then an overview of the closed loop control techniques is discussed for the bidirectional dc-dc converter. The average mode current control (AVGCCM) two-loop method was selected to test the functionality and accuracy of the six phase interleaved converter by using mid-point sampling, while a different unified bidirectional control technique is proposed for the mode transition. The AVGCCM technique is shown to achieve equal current sharing of all six phases and it is tested experimentally up to 4.88kW. The unified bidirectional control technique was tested with 12V and 24V batteries on each side of the converter to validate the transition of both boost-to-buck and buck-to-boost modes of operation.

II. INTERLEAVING DC-DC BOOST CONVERTER

Fig. 1 shows the proposed six phase interleaved bidirectional converter. As with many multiphase converters, equal current sharing is a primary requirement when

interleaving multiple phases. Many interleaving techniques have been proposed in the literature. Most use a current control loop for each phase, which adjusts the duty cycle to achieve the required phase current [5-7]. By controlling each phase current, equal current sharing can be achieved during interleaving. Fig. 2 shows the equal and unequal current sharing cases for six-phase operation. Clearly, when there is unequal current sharing, each phase will carry a different amount of current and as a result, the losses and, in turn, heat dissipation will become unbalanced, since one phase will be carrying more current than another.
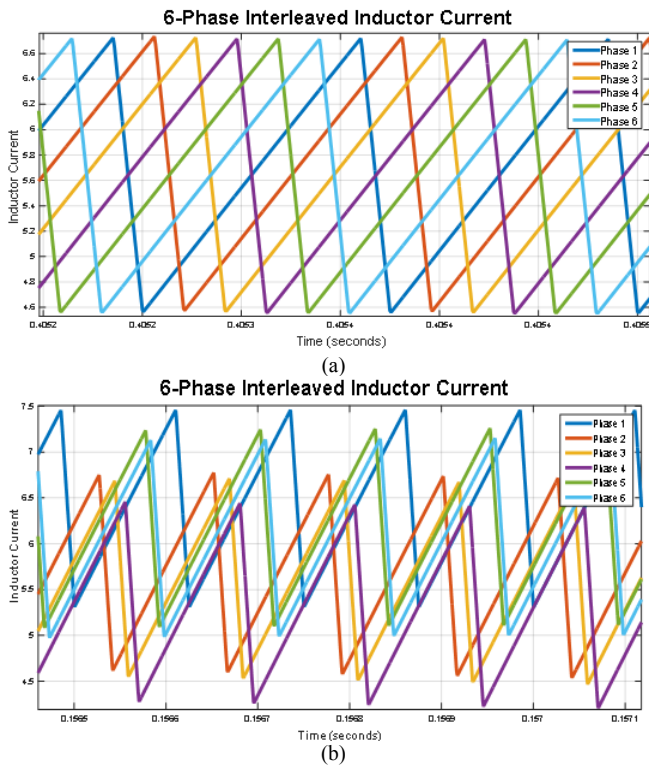

(a)

(b)

Fig. 2.   Current sharing in six-phase operation (a) equal current sharing (b) unequal current sharing.

One way uneven current sharing occurs is due to improper sampling. When interleaving multiple phases, each phase is shifted by T_s / N where Ts is the period and N is the number of phases. Because of this phase difference, at each moment in time the phase currents in each phase will also be different. Therefore, if all phase currents were sampled at the same point in time, each phase would then have different current values. Therefore, the sample locations of each individual phase must also be taken at different moments in time. Fig. 3 shows mid-point and peak-point sampling, which can be used to sample the phase currents at individual moments in time. This ensures that each phase sample is equivalent to each other. Each dot in Fig. 3 indicates a sample point for a specific phase. For example, the first dot in Fig. 3 (a) is the sample point for phase six only, while the second dot is the sample point for phase one only and so on. If the first dot was used to sample all phase currents, there would be a difference between the sampled values of each phase current. If a current control loop is used to

control the converter, the duty cycle of the switches is directly dependent on the difference between the phase current and the reference current. As such, if each phase current is different, the duty cycle will be different, and uneven current will result as shown in Fig. 2 (b). Thus, there needs to be a common sampling location for each phase to prevent this problem.
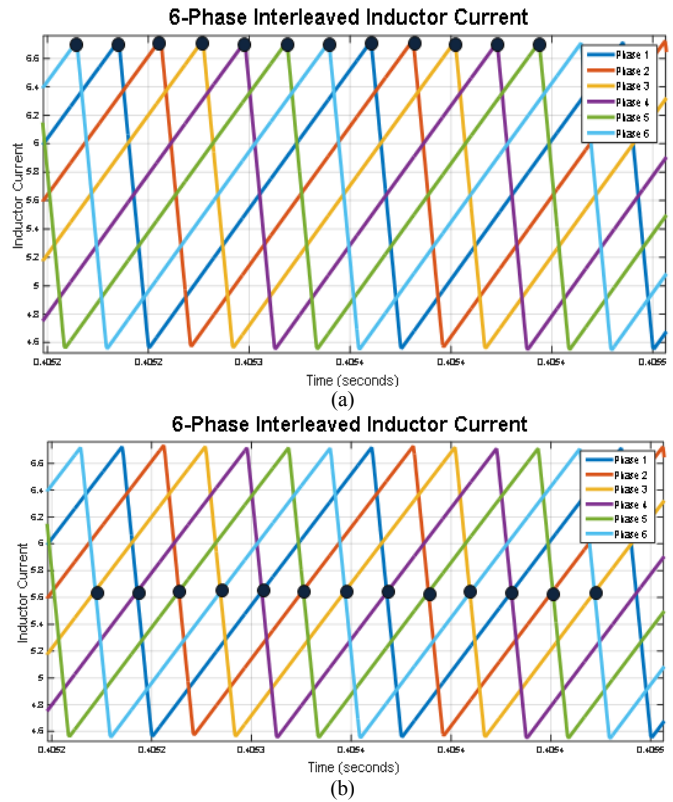

(a)

(b)

Fig. 3.   Current sharing in six-phase operation (a) mid-point sampling (b) peak sampling.

Another important consideration is to ensure that the duty cycle PWM and the sample points are synchronized. This means that, the sample point should always be at a specific location in reference to the PWM. Otherwise, there will be a delay or disturbance within the system. If the sampling clock is not synchronized to the PWM generation, the condition in Fig. 2 (b) could occur, due to the difference in sampling time. By sampling the phase current at a specific PWM event, such as a rising edge or falling edge, the PWM can be synchronized with the sampling instant. Fig. 4 shows the synchronization between the sample times (vertical red lines), PWM carrier (blue
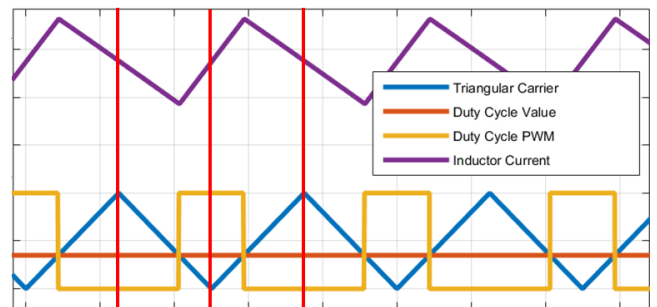

Fig. 4.   Mid-point sampling/triangular carrier PWM synchronization

triangular pulse), and duty cycle value (horizontal red line D=0.2) for mid-point sampling of a single phase. In most interleaved applications each phase has its own current sensor to measure the inductor current, but there are applications where only one current sensor can be used as in [7]. However, when using a single current sensor at the output, there will be a limit on the duty cycle range since the output current is a combination of each phase.

III. AVERAGE MODE CURRENT CONTROL

There are many different types of converter control techniques throughout literature ranging from voltage mode [9-11], current mode [9-13], sliding mode [14-18], and fuzzy logic control [19-20]. In this paper the Average Mode Current Control (AVGCCM) technique is utilized for its simplicity of implementation, and improved dynamics and stability compared with single loop control [11].
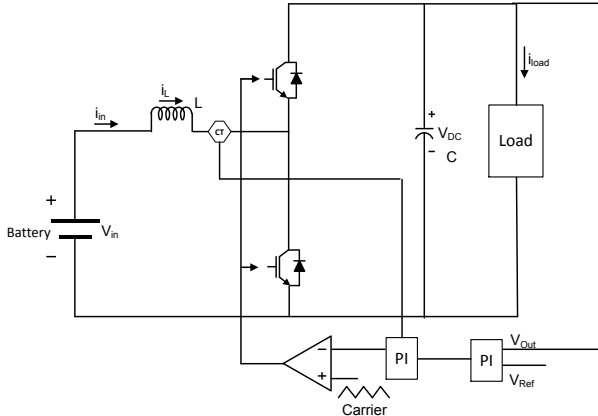

Fig. 5.   Average Mode Current Control.

Fig. 5 shows the proposed AVGCCM technique in a single-phase converter and it can easily be extended to six or more phases. The output voltage is measured and compared with the reference value. The difference between these values is then sent to a voltage loop PI controller, which calculates the desired inductor phase current to achieve the output voltage reference. The desired current is then compared with the measured phase current and the error is sent to the current loop PI controller. Here the duty cycle value is determined to achieve the desired inductor phase current. This duty cycle value is then compared with a fixed frequency triangular carrier waveform, generating the PWM waveform for the switches. By controlling the switches, the current and voltage will change. Therefore, depending on the duty cycle value, a specific inductor current and output voltage can be maintained.

IV. BIDIRECTIONAL CONTROL

One way to achieve bidirectional power flow is to have two separate controlers which are switched on or off depending on which mode of operation is required [21]. However, syncronous rectification can be utilized to control both switches and hence, have a single controller for both modes

[21-23]. This paper proposes a unified controller using synchronous rectification for both modes of operation. The main advantage of using synchronous rectification is the elimination of the discontinuous conduction mode (DCM), reduce voltage and current stress during mode transition, and inductor voltage parasitic ringing [21]. The proposed bidirectional controller is shown in Fig. 6. Only one phase is depicted; however, interleaving multiple phases can easily be done. The main idea behind this technique is to control the inductor current in both directions. By controlling the inductor current, both modes of operation can easily be implemented. Looking at Fig. 6, a negative current reference indicates current flowing out of the battery, hence boost operation, while a positive current reference indicates current flowing into the battery, and hence buck operation. Thus, to adjust the inductor current, the inductor voltage can also be controlled.
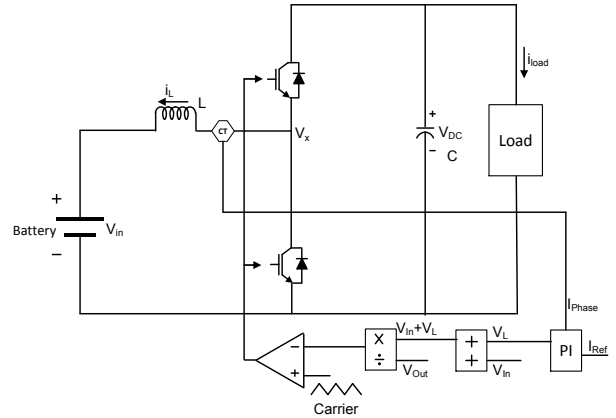

Fig. 6.   Single phase bidirectional converter.

Equation (1) relates the inductor current to the inductor voltage and inductance:

$$L\frac{di_L}{dt} = V_L \tag{1}$$

The KCL equation of Fig. 6 during the off-time of the bottom switch is shown in (2). It relates the inductor voltage, V_L, to the input voltage, V_{in}, and voltage across the bottom switch, V_x,

$$V_L = V_x - V_{in} \tag{2}$$

Subsituting (2) into (1),

$$L\frac{di_L}{dt} = V_L = V_x - V_{in} \tag{3}$$

Over one switching cycle the voltage across the bottom switch is,

$$V_x = \begin{cases} 0 & 0 < t < DT_s \\ V_0 & DT_s < t < 1 \end{cases} \tag{4}$$

where D is the duty cycle of the bottom switch and Ts is the switching period. Subsituting (4) into (3) during Toff gives,

$$L\frac{di_L}{dt} = V_L = DV_o - V_{in} \tag{5}$$

Rearanging (5) and solving for D,

$$D = \frac{V_L + V_{in}}{V_o} \tag{6}$$

Now the duty cycle of the bottom switch is related to the inductor voltage; therefore, the inductor current can be changed by adjusting the duty cycle and measuring the output voltage and input voltage. The controller measures the inductor phase curent and compares it with the reference current.
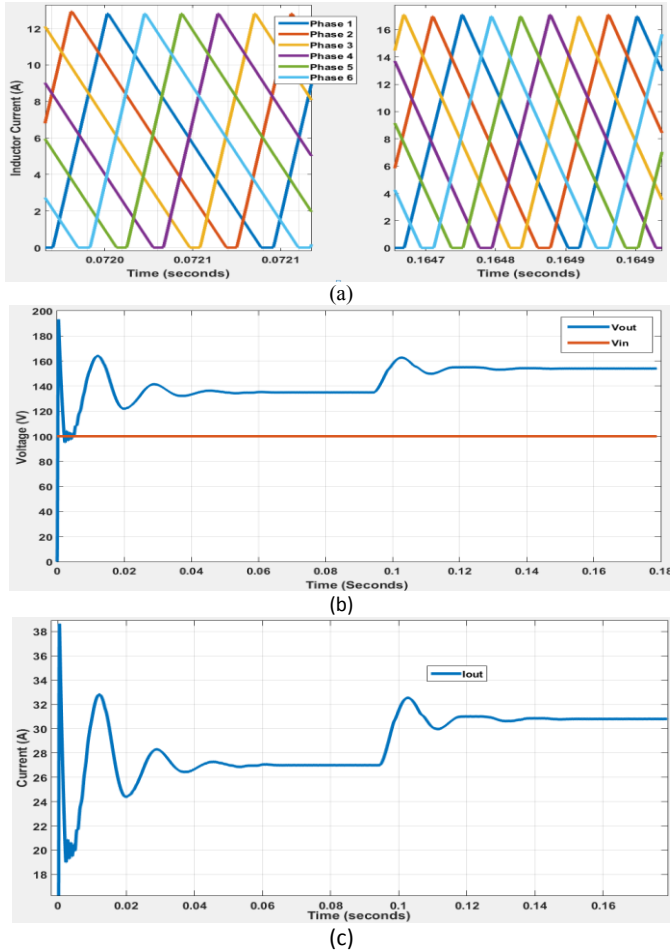

(a)

(b)

(c)

Fig. 7.   Matlab/Simulink Simulation. (a) Inductor current at vout references of 135V and 154V (b) Vout and Vin (c) Iout.
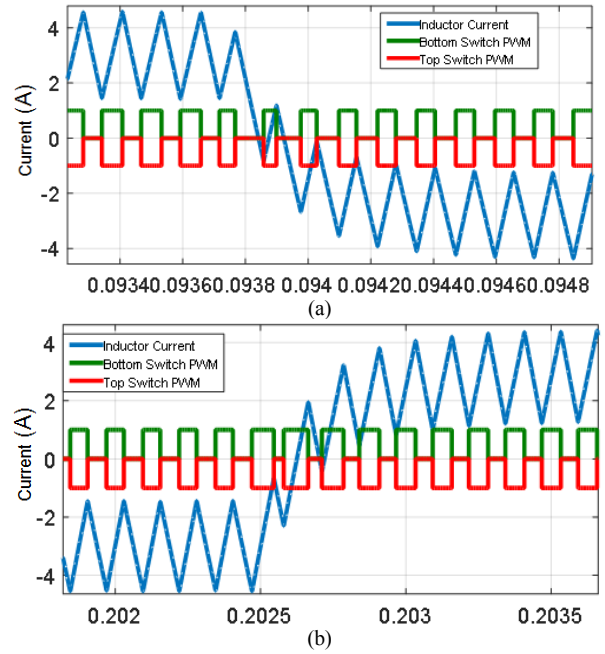

(a)

(b)

Fig. 8.   Mode transitions (a) boost to buck (b) buck to boost.

The error is sent to a current loop PI controller which calculates the required inductor voltage to achieve the desired current. The inductor voltage is then used in equation (6) and is added to the input voltage measurement and divided by the output voltage measurement to determine the required duty cycle value of the bottom switch to realize the current refrence. This duty cycle value is then compared to a constant frequncy triangular carrier waveform to generate the PWM duty cycle for the top and bottom switches. The AVGCCM control is shown in Fig. 7 while the bidirectional control is shown in Fig. 8 under the test conditions in Table I. Both controllers were simulated using Matlab/Simulink. It is clear that the inductor current is in CCM operation at all times while achieving no large transients during the transition in Fig. 8. The values of the top and bottom duty cycles can be ignored as they are only shown to visiualize the relationship between the switching times and the inductor current waveform in blue.

V. RESULTS

Fig. 9 shows the test setup of the six-phase interleaved bidirectional converter. In this paper the six-phase interleaved converter is tested at low and high power using AVGCCM. The converter is to be tested at 8 kHz; therefore, each phase is separated by 20.833 μs as discussed in Section I, to achieve proper interleaving and equal current sharing. The control of the converter was done using the TI DSP TMS320F28335. Fig. 10 shows equal current sharing of the six-phase interleaved bidirectional converter using AVGCCM under low power conditions specified in Table I. Fig. 11 (a) shows the high power testing waveforms at 3.79 kW and Fig. 11 (b) shows the test at 4.88 kW, under AVGCCM using all six

TABLE I
EXPERIMENTAL PARAMETERS AND TEST

AVGCCM at Low Power			
Input Voltage (V)	Output Voltage (V)	Output Capacitor (uF)	Output Resistance (Ω)
5	30	514	5
Input Inductor (uH)	Switching Frequency (Hz)	Voltage PI	Current PI
240	8000	Kp=0.01, Ki=5	Kp=0.0005, Ki=0.00001
AVGCCM at High Power			
Input Voltage (V)	Output Voltage (V)	Output Capacitor (uF)	Output Resistance (Ω)
100-120	130-150	514	5
Input Inductor (uH)	Switching Frequency (Hz)	Voltage PI	Current PI
240	8000	Kp=0.01, Ki=5	Kp=0.0005, Ki=0.00001
Unified Bidirectional Converter			
Input Voltage (V)	Output Voltage (V)	Output Capacitor (uF)	Input Inductor (uH)
12	24	514	240
Switching Frequency (Hz)	Current Reference During Boost(A)	Current Reference During Buck(A)	Current Pi
8000	-3	+3	Kp=0.2, Ki=0.8

phases. For simplicity only one phase was shown in operation; however, all six phases are operating under equal current sharing as intended during these tests and shown through simulation in Fig. 7 and Table I. Fig. 12 shows the bidirectional boost converter using the unified controller under steady state operation in boost mode in (a), steady state buck mode in (b), and boost to buck mode transition in (c). For simplicity only one mode transition is shown since both have very similar responses.

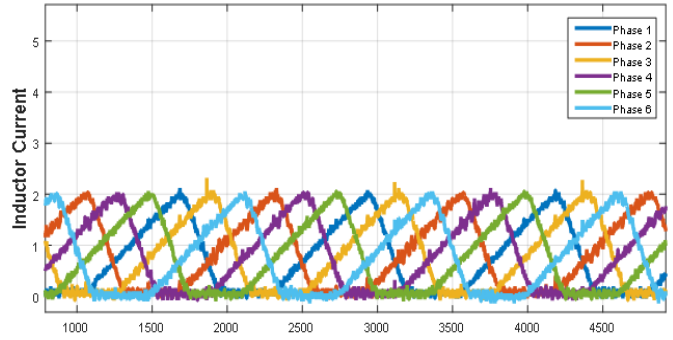Fig. 9.   Six-phase Bidirectional Test Setup.

Fig. 10.   Inductor current waveforms in boost mode using AVGCCM

In Fig. 12, the 12-volt input battery current is represented by the purple plot while the 24-volt output battery current is the green plot. The input current is negative during boost mode and positive during buck mode as specified by the test conditions in Table I. To test the mode transitions, the reference current was changed between positive and negative three amps indicated by the purple and green ripple values in Fig. 12. It is clearly shown that during this transition, CCM is achieved, indicated in Fig. 12 by the bottom switch duty cycle in blue. There is also no large voltage or current transients during these transitions providing safe operation.
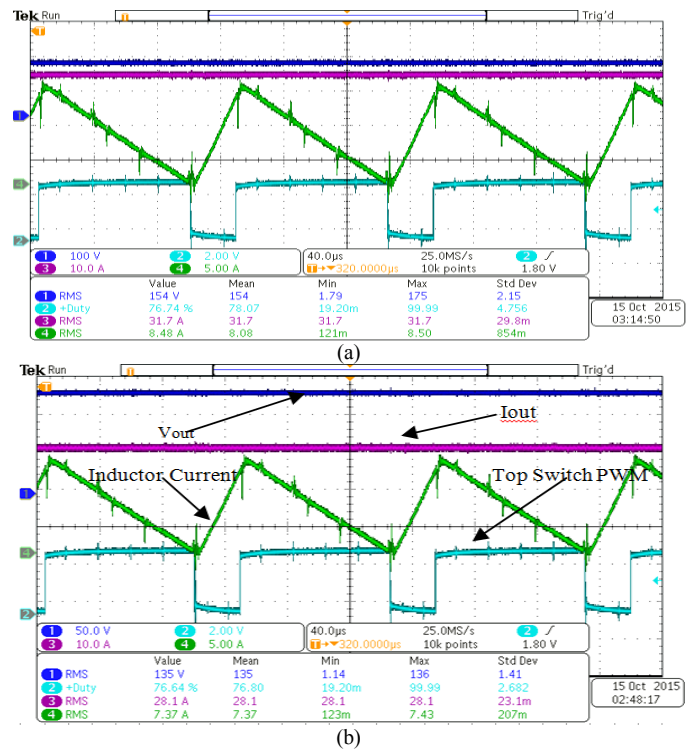

(a)

(b)

Fig. 11.   High power testing using AVGCCM in boost mode under conditions in TABLE I. (a) 4.88kW, (b) 3.79kW.
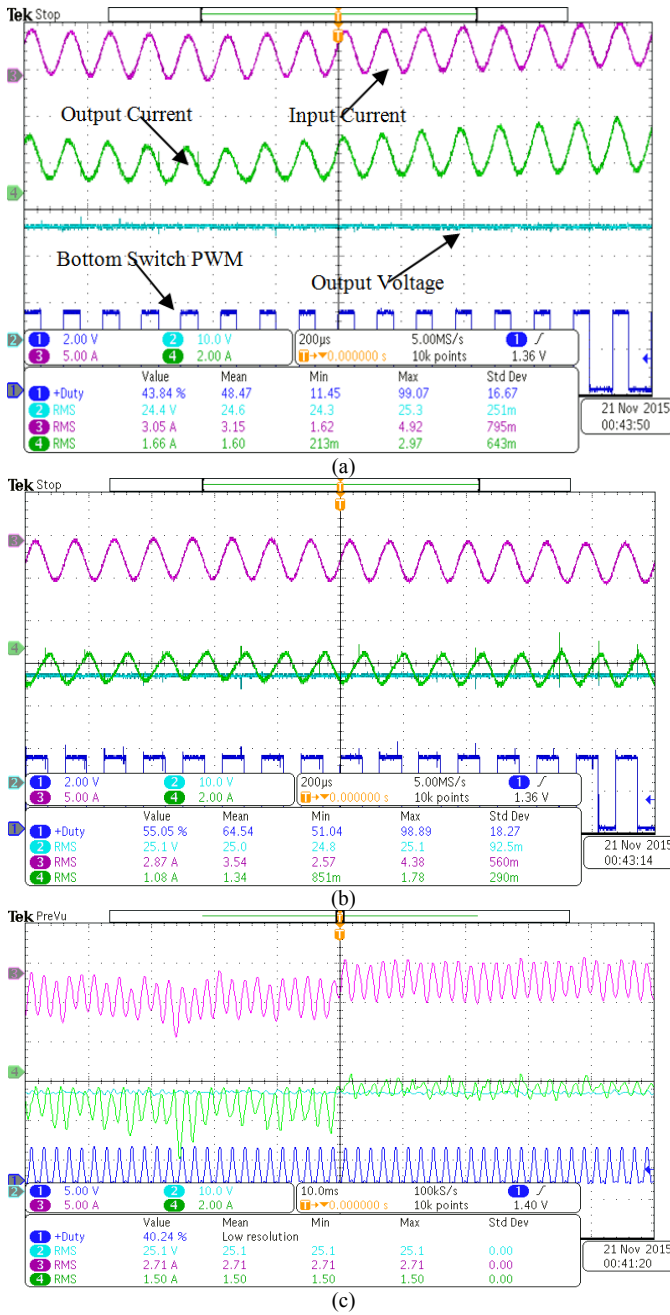
Fig. 12. Single phase battery testing using unified controller (a) steady state boost mode (b) steady state buck mode (c) boost to buck mode transition.

VI. Conclusion and Future Work

This paper presents the AVGCCM technique for a six phase interleaved bidirectional converter and also a unified controller for the bidirectional mode transition. The AVGCCM technique has been shown to have equal current sharing under low and high power test conditions of the six phase bidirectional converter while maintaining an output voltage reference specified in Table I. The unified controller has also been tested with 12-volt and 24-volt batteries on either side of the converter to validate the transition of both boost-to-buck and buck-to-boost modes of operation. The transition between boost and buck modes has been shown to maintain an inductor phase current reference of negative and positive three amps while achieving continuous conduction mode during the mode transitions. It was also shown that there were no large transients during the mode transitions in either direction. To test the bidirectional operation, only one phase was implemented using batteries because of the limitation in power provided from the batteries. Thus, the next steps would be to test the transition between each operation mode using higher power batteries or by using a bidirectional power supply.

References

[1] P. Magne, P. Liu, B. Bilgin, and A. Emadi, "Investigation of impact of number of phases in interleaved dc-dc boost converter," in *Proc. IEEE Transportation Electrification Conference and Expo*, Dearborn, MI, June 2015, pp. 1-6.

[2] S. Lu, K. A. Corzine, and M. Ferdowsi, "A new battery/ultracapacitor energy storage system design and its motor drive integration for hybrid electric vehicles," *IEEE Transactions on Vehicular Technology,* vol.56, no.4, pp.1516-1523, July 2007.

[3] K. W. Hu, P. H. Yi, and C. M. Liaw, "An EV SRM drive powered by battery/supercapacitor with G2V and V2H/V2G capabilities," *IEEE Transactions on Industrial Electronics,* vol.62, no.8, pp.4714-4727, Aug. 2015.

[4] M. Marchesoni, and C. Vacca, "New dc–dc converter for energy storage system interfacing in fuel cell hybrid electric vehicles," *IEEE Transactions on Power Electronics,* vol.22, no.1, pp.301-308, Jan. 2007.

[5] L. Ni, D. J. Patterson, and J. L. Hudgins, "High power current sensorless bidirectional 16-phase interleaved dc-dc converter for hybrid vehicle application," *IEEE Transactions on Power Electronics,* vol.27, no.3, pp.1141-1151, Mar. 2012.

[6] J. Sun, "Dynamic performance analyses of current sharing control for dc/dc converters," Ph. D. dissertation, Virginia Tech, June 13, 2007.

[7] H. Higure, N. Hoshi, and J. Haruna, "Inductor current control of three-phase interleaved DC-DC converter using single DC-link current sensor," in *Proc. IEEE International Conference on Power Electronics, Drives and Energy Systems,* Bengaluru, India, Dec. 2012, pp.1-5.

[8] O. Garcia, P. Zumel, A. D. Castro, and J. A. Cobos, "Automotive dc-dc bidirectional converter made with many interleaved buck stages," *IEEE Transactions on Power Electronics*, vol.21, no.3, pp.578-586, May 2006.

[9] S. He, J. Y. Hung, and R. M. Nelms, "Small-signal modeling of I^2 average current mode control," *IEEE Transactions on Power Electronics,* vol.31, no.5, pp.3849-3858, May 2016.

[10] K. Wan, "Advanced current-mode control techniques for dc-dc power electronic converters," Ph. D. dissertation, Missouri University of Science and Technology, 2009.

[11] L.H. Dixon, "Average current-mode control of switching power supplies," Unitrode Power Supply Design Seminar handbook, pp. 5.1-5.14, 1990.

[12] C.M. Franklin, B.A. McDonald, and J.C. Vogt, "Digital peak current mode control for switched-mode power converters," U. S. Patent 8,773,097, July 2014.

[13] G. Garcera, E. Figueres, and A. Mocholi, "Novel three-controller average current mode control of dc-dc pwm converters with improved robustness and dynamic response," *IEEE Transactions on Power Electronics,* vol.15, no.3, pp.516-528, May 2000.

[14] L. Shen, D. D. -C. Lu, and C. Li, "Adaptive sliding mode control method for dc-dc converters," *IET on Power Electronics,* vol.8, no.9, pp.1723-1732, Sept. 2015.

[15] Y. He, and F. L. Luo, "Sliding-mode control for dc-dc converters with constant switching frequency," *IEE Proceedings on Control Theory and Applications,* vol.153, no.1, pp.37-45, 16 Jan. 2006.

[16] R. J. Wai, and L. C. Shih, "Design of voltage tracking control for dc-dc boost converter via total sliding-mode technique," *IEEE Transactions on Industrial Electronics, v*ol.58, no.6, pp.2502-2511, June 2011.

[17] M. Salimi, J. Soltani, A. Zakipour, and N. R. Abjadi, "Hyper-plane sliding mode control of the dc-dc buck/boost converter in continuous and discontinuous conduction modes of operation," *IET on Power Electronics,* vol.8, no.8, pp.1473-1482, Aug. 2015.

[18] R. Ling, D. Maksimovic, and R. Leyva, "Second-order sliding-mode controlled synchronous buck dc-dc converter," *IEEE Transactions on Power Electronics,* vol.31, no.3, pp.2539-2549, March 2016.

[19] A. R. Ofoli, and A. Rubaai, "Real-time implementation of a fuzzy logic controller for switch-mode power-stage dc-dc converters," *IEEE Transactions on Industry Applications*, vol.42, no.6, pp.1367-1374, Nov.-Dec. 2006.

[20] A. G. Perry, F. Guang, Y. F. Liu, and P. C. Sen, "A design method for pi-like fuzzy logic controllers for dc-dc converter," *IEEE Transactions on Industrial Electronics, v*ol.54, no.5, pp.2688-2696, Oct. 2007.

[21] J. Zhang, "Bidirectional dc-dc power converter design optimization, modeling and control", Ph.D. Dissertation, Virginia Polytechnic Institute and State University, Jan. 30, 2008.

[22] A. S. Samosir, and A. H. M. Yatim, "Implementation of dynamic evolution control of bidirectional dc-dc converter for interfacing ultracapacitor energy storage to fuel-cell system," *IEEE Transactions on Industrial Electronics,* vol.57, no.10, pp.3468-3473, Oct. 2010.